We are IntechOpen,
the world's leading publisher of
Open Access books
Built by scientists, for scientists

6,900
Open access books available

186,000
International authors and editors

200M
Downloads

Our authors are among the

154
Countries delivered to

TOP 1%
most cited scientists

12.2%
Contributors from top 500 universities

CLARIVATE ANALYTICS
BOOK CITATION INDEX
INDEXED

WEB OF SCIENCE™

Selection of our books indexed in the Book Citation Index
in Web of Science™ Core Collection (BKCI)

Interested in publishing with us?
Contact book.department@intechopen.com

Reliability and Lifetime Prediction for IGBT Modules in Railway Traction Chains

X. Perpiñà[1], L. Navarro[1], X. Jordà[1], M. Vellvehi[1],
Jean-François Serviere[2] and M. Mermet-Guyennet[2]
[1]IMB CNM CSIC, Barcelona,
[2]Alstom Transport, Tarbes
[1]Spain
[2]France

1. Introduction

Electric railway traction chains (ERTCs) emerged at the end of the nineteenth century. Over the years, they have been consolidated as a better solution than their counterparts, i.e., the traction systems with generating power on board (e.g., diesel or steam-based systems). In terms of performances, ERTCs show the highest power-to-weight ratio, fastest acceleration and highest traction effort on steep gradients of the railway traction scenario. They also offer other advantages; such as: less noise, lower maintenance requirements of the traction units, and a higher rational use of energy respecting and preserving the environment (e.g., energy harvesting systems as regenerative brakes or no greenhouse gasses' emissions). However, their drawback is the electrification line cost, which always entails an economical viability study according to a trade-off between line distance and volume traffic. When this investment is not economically profitable, the optimum solution is a hybrid approach combining generating power on board (based on fossil fuels) and electric engines.

Such figures of performance for ERTCs would not be possible without power electronics development. As a matter of fact, ERTCs are based on power conversion strategies (power converters), which use semiconductor power devices. Power converters are electrical circuits which supply the energy from high voltage electrified lines (DC voltage from 1.5 to 3 kV or AC voltage of 25 kV at 50 Hz) to railway motors (2800-8800 kW) by using semiconductor power devices, passive elements (e.g., DC link capacitors), and mechanical actuators (e.g., circuit breaker). In this framework, semiconductor power devices are responsible for diverting and switching the electrical current (rectifiers and power switches, respectively) among the different branches of the power converter, supporting high current and voltage ratings under working conditions. Such extreme working conditions fix their reliability problems, since they usually arise either from the ruggedness of such devices to non-desired electrothermal events (Perpiñà et al., 2007a, 2010a) (e.g., short-circuit, overvoltage, overcurrent, or overtemperature) or from the ageing of one of the power converter constituting elements (Ciappa, 2002; Malagoni-Buiatti et al., 2010) (e.g., capacitors, bus bar or power device packages). Both phenomena have a negative effect on power devices: their working conditions become more adverse (overload conditions in terms of

current, voltage or temperature), eventually causing their explosion. Thus, a complete knowledge of the physical signature of their failure not only could provide precious information about its cause, but also could reveal the origin of the overloading condition. For this reason, a good comprehension of this topic is desired by ERTC manufacturers. Several efforts have been invested in investigating (e.g., projects LESIT, PORTES, etc.) which is the impact on the converter long-term reliability when the packaging of power devices (multi-chip power module) wears out and/or when such power devices fail. In fact, this is one of the main hot topics in the current research in the fields of railway traction and power devices design for reliability.

This chapter presents and revises this problematic issue, eventually proposing an approach for the determination of the most thermo-electrically stressed devices of a power converter. For this purpose, this chapter will be organised as follows: Section 2 provides a description of ERTC parts, also introducing their reliability problems. Section 3 presents the most used power devices for railway applications and their packaging technology, highlighting the packaging wear-out problems. The lifetime prediction methodology currently used in railway traction is critically reviewed in Section 4, stressing their main limitations and challenges. In the last two sections, an experimental approach based on determining local thermal stresses within the package is proposed. This work has been performed in the framework of a European funded program called PORTES (*POwer Reliability for Traction ElectronicS*) (Portes, 2004), mainly devoted to explore and understand the physical failure mechanisms for the first generation of IGBT power modules.

2. ERTC description and reliability problems

Fig. 1 depicts an ERTC schematic, in which the energy delivery process to the motor can be followed. By using a line contactor (pantograph or floaters), the energy is extracted from an external source (electrified lines or catenary) and it is adapted by several power conversion strategies until arrive to the electrical traction motors. The final conversion stage is performed by the motor drives or inverters (see Fig. 1), which consist in a DC-AC converter (Mohan et al., 1995). They drive the train electrical engine (train speed control and braking) (Mermet-Guyennet et al., 2007) using IGBT (Insulated Gate Bipolar Transistors) multi-chip power modules, in which IGBT devices and freewheeling diodes are packaged together (multi-chip packaging strategy). In this application, the IGBTs are switched according to a pulse-width-modulation pattern (i.e., between 200 Hz and 2 kHz, indicatively) (Mohan et al., 1995) to supply the required sinusoidal input current to the motor (inductive load); whereas the freewheeling diodes ensure a continuous path for the current coming from the motor (Mohan et al., 1995). Fig. 1 also shows a schematic of a 3-phase power inverter for driving traction motors: it is formed by three branches or legs, which contain two IGBT modules each one (M_x in Fig. 1). The motor is represented by three inductive loads interconnected to the nodes between IGBT modules. Aside from IGBT modules, they also include a cooling system (based on air-forced convection, heat-pipes or liquid pump technologies) (Bouscayrol et al., 2006; Baumann et al., 2001), bus-bar high power connections, a close control command or IGBT drivers for switching them (Steimel, 2004;), low voltage connections, capacitors (decoupling or filtering) (Malagoni-Buiatti et al., 2010), mechanical parts for support and connectors, and a control board and current sensors integrated in the IGBT module (Bose, 2006).
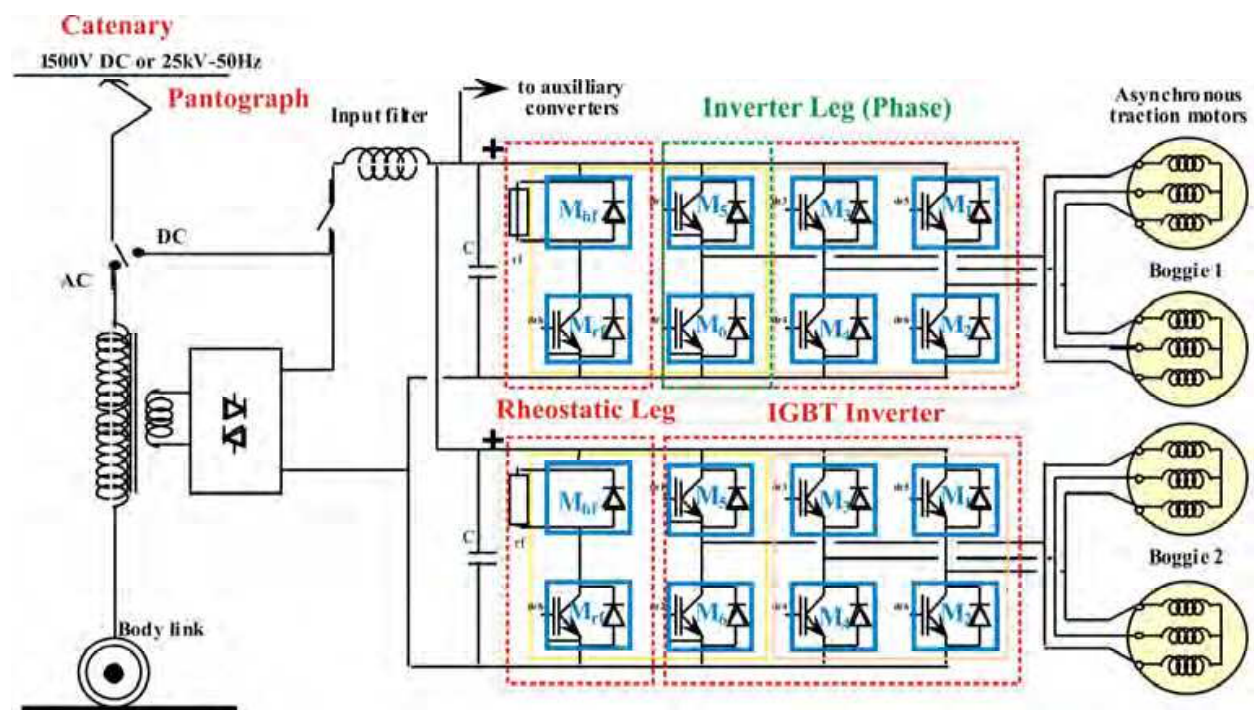
Fig. 1. Example of an ERTC showing the external supply line, a circuit breaker which connects the required conversion scheme, a first power conversion stage when an AC supply line is employed (AC-DC converter in this case), the body link, two 3-phase inverters, two choppers, and electrical motors. Special emphasis is put on the electrical connections within the 3-phase inverters.

Within ERTCs, the power inverter represents the most stressful application scenario for power devices, since it has an inductive load and this impose severe working conditions during the IGBT turn-off or diode reverse recovery (coexistence of high voltage and current levels in both cases). Therefore, the key points to achieve a satisfactory design for reliability of power inverters are (Mohan,1995):

- *Safe operating area*: the voltage and current of IGBT modules must remain within the limits given by their manufacturer under operating conditions.
- *Dielectric requirements*: the high voltage operation imposes minimum distances among the materials within the package to avoid dielectric breakdown and partial discharges.
- *Thermal limits*: the designer verifies that for a train duty cycle representative of a service line (mission profile), the working temperature and its variations (temperature swing) does not exceed certain maximum values.

This last aspect requires an accurate estimation of the train duty cycles or mission profiles, the IGBT and diode junction temperatures, and the behaviour of IGBT power modules under thermal cycles. Such thermal cycles come from the actual working conditions of the packaged devices: their selfheating (Arnold et al., 1994) induce a temperature field inside the IGBT module, which evolves depending on the train speed along a railway service line. Consequently, the power module experiences several local thermal cycles defined by the train acceleration and braking processes (Coquery et al., 2003) that, in turn, provokes local stresses among such materials because they show different thermal expansion coefficients (CTE). This leads to the apparition of crack propagation or interface delamination of the

solder joint of the package assembly, which will locally increase the thermal resistance of the power module (thermal performance degradation) (Ciappa, 2002). During this process, there is another aspect that has an important role: the thermal contact between the power module and the cooling system. A perfect thermal contact between an IGBT power module and its cooling system is not always assured all over the module backside (uneven thermal resistance along the module backside), as evidenced in (Hamidi, 1998a; Perpiñà et al., 2010b). Then, the addition of both effects can provoke that some components reach temperature values, which lead to their destruction by burn-out (Sankaran et al., 1997; Ciappa, 2002; Perpiñà et al., 2010a).

The packaging wear-out due to thermo-mechanical effects was extensively studied in the nineties, particularly through the research programs called LESIT (*LeistungElektronik Systemtechnik InformationsTechnologie*, 1994-1997) and RAPSDRA (*Reliability of Advanced high Power Semiconductor Devices for Railway traction Applications*, 1996-1998). They led to the definition of Power Cycling Tests (PCTs) and lifetime prediction methods for railway traction IGBT modules (Hamidi et al., 1998b), that will be presented further on. Up to then, thermal cycling was the most common approach for accelerating the IGBT modules' ageing: the whole power module was submitted to the same temperature swings following square waveforms with different thermal profiles (duty cycles) in a temperature-controlled chamber (Bouarroudj et al., 2008; Lhommeau et al., 2007). The problem of this test was that the local thermal stress induced by power devices was not taken into account. Therefore, this approach was not suitable for wear-out studies of power modules and lifetime prediction from the final application viewpoint. However, power thermal cycling presents some limitations, as will be further discussed in Subsection 4.2:

- it deals with a macroscopic approach for lifetime prediction (average temperature values of the module) and do not determine the most thermally stressed devices for a given cooling system,
- it does not reproduce the power module failure under a real working condition, i.e., high current and voltage ratings.

Therefore, promoting thermal studies at chip level is fundamental for a better understanding of ERTC failures and for increasing its lifetime (Coquery et al., 2001). In fact, the key point is to monitor the temperature inside a power module under a thermal working condition representative of the final application. In these studies, one of their main goals should be verifying whether reliable operating and uniform temperatures are assured within a power module. With these tests, dysfunctions on cooling systems behaviour or non-reliable thermal designs of multi-chip modules would be evidenced. Besides, this information will contribute to the knowledge of the local influence of the temperature distribution on the devices assembled within the module, since there is a lack of experimental results reported in the literature.

3. Multichip power modules for railway traction

The current generation of power inverters for railway traction is based on the use of high voltage IGBT (*Insulated Gate Bipolar Transistor*) power modules (Rahimo et al., 2004). They consist in multi-chip devices (IGBTs and diodes) integrated in the same package, which cover a large range of voltage (1700V, 3300V, 6500V) and nominal currents (1600A-2400A,

1200A, 600A). This package, electrically interconnects several power semiconductor devices, extracts the dissipated heat through a thermal path separated (or not) from the electric path, isolates the high voltages from other critical parts of the system, and provides a mechanical support to the devices. In this framework, power electronics packaging plays an important technical and economical role, because it constitutes the interface between the raw semiconductor device and the circuit application. In this section, its main parts will be explained in Subsection 3.1, the semiconductor devices usually employed in railway applications will be briefly presented in Subsection 3.2, and its ageing mechanisms will be revised in Subsection 3.3.

3.1 Power electronics package and IGBT multi-chip power module structure

Fig. 2 shows the structure of a typical power electronics package for a single (discrete) or multiple (multi-chip module) dies, whose main constitutive elements are (Sheng & Colino, 2005):

- *Power semiconductor devices* (IGBT, FRED). They provide the current flow control function previously described.
- *Die-attach technology*. It contacts the die to the substrate mechanically, electrically and thermally.
- *Top-side interconnections*. They perform the electrical contact on the device top-side. In some cases, they can also provide top heat extraction (e.g., bump interconnection technology).
- An *electrically insulating and thermally conductive substrate*. It is the mechanical support of the devices, tracks and terminals, as well as it permits the electrical insulation between some of them. It also provides an efficient heat extraction path.
- An *encapsulating material*. Typically it consists on a conformal coating or casting for environmental and mechanical protection.
- *A base plate*. It provides a mechanical support, as well as it favors both the spreading and conduction of heat towards the cooling system.
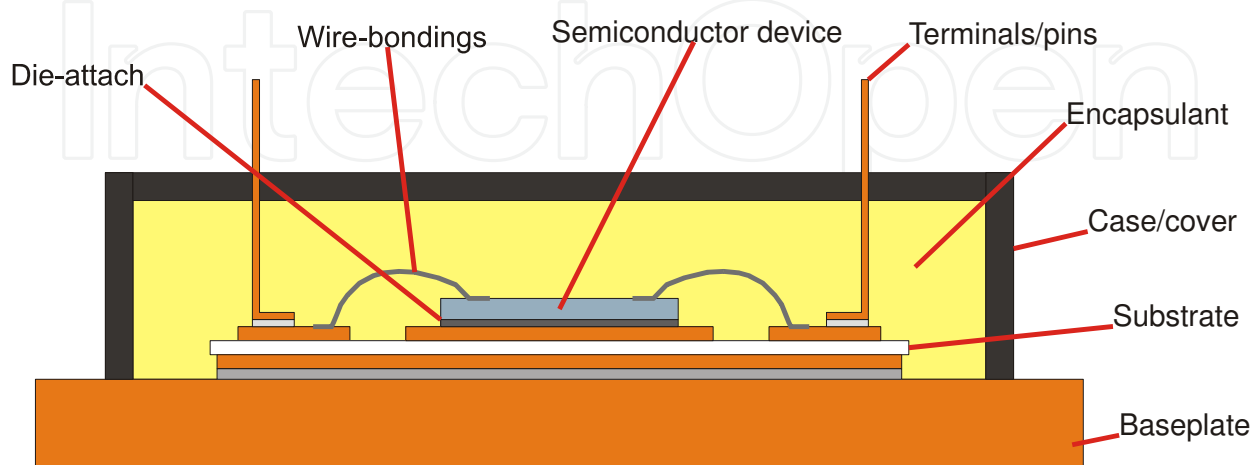- *Case and cover*. It is a housing structure that protects all devices and interconnections.

Fig. 2. Typical power electronics package structure.

Each one of these constitutive elements is made of a certain material depending on its functionality and position within the package. The material selection is performed according to its physical properties (electrical resistivity, thermal conductivity, or mechanical properties) to meet the package requirements. Typical materials used in power packaging are:

- *Power semiconductor devices*. Mainly silicon-based devices, although other semiconductors have been also introduced (SiC JFETs and rectifiers, AlGaN/GaN HEMTs, AsGa diodes).
- *Electrically insulating/thermally conductive substrate*. Usually ceramic substrates are (Al_2O_3, AlN, Si_3N_4, BeO) with copper layers on top and backside. The typical technology in railway power modules is the DCB (Direct Copper Bonded). For low and medium power ratings, metal (typically aluminum) substrates with a ceramic-filled polymer (typically epoxy) layer are used instead of the ceramic ones (e.g., Insulated Metal Substrate –IMS- technology).
- *Base plate*. Typically, they are based on nickel plated copper slabs. Other materials are metal matrix composites such as copper matrix composites reinforced with diamond, aluminum matrix reinforced with SiC, carbon-reinforced composites, etc.
- *Die-attach*. The usual solder joint material is the PbSnAg alloy, but now other lead-free alloys are used or new materials, such as Silver nano-sintering, have also been introduced.
- *Top-side interconnections*. The most used technique is large aluminum wire-bonding. Other solutions include pressure-type contact and metal bumps.
- *Case and cover*. Thermoset and thermoplastic materials including silicones and epoxies.

In order of importance, the package starts at the interface of the chip itself (first level packaging) and extends to higher levels of integration; such as substrate-level and system-level. The first level consists in the attachment of one or more bare chips to a substrate, the interconnection from these chips to the package leads, and the encapsulant (cover). The first level interconnection has a major role, because it directly interfaces with the chips, not only electrically, but also thermally and mechanically. For reducing the thermal stresses in the chips, it is necessary a thermal-friendly interconnection design. And lastly, the reliability of the first level interconnection is vital to ensure an extended lifetime of the electronic assemblies. At this point, a good thermo-mechanical matching property (mainly the CTE) between neighboring materials is crucial, as will be discussed in Subsection 3.3. Other aspects taken into account for their design are the optimization of the electrical circuit of the package (parasitic inductance and resistance reduction), its electromagnetic compatibility (low parasitic radiation and conduction), the mechanical roughness, and the package thermal management.

In the case of IGBT power modules, the chips are typically connected by wire-bonding technology. In such modules, a DCB substrate is commonly used as a ceramic substrate for the power device. DCB provides an excellent electrical insulation as well as good thermal conduction due to the direct bonding of copper on ceramic materials; such as alumina and aluminum nitride. The materials used for device and DCB attachment are usually solder alloys. Fig. 3 (a) shows a commercial 3.3kV IGBT module, and Fig. 3 (b) shows the chip interconnection within the modules. Their internal structure consists of three elementary phases (A, B, and C) according to the distribution of the anode (collector) and cathode

(emitter) power terminals, as depicted in Fig. 3 (a). Each elementary phase includes eight IGBTs (T_x in Fig. 3 (a)) and four free-wheeling diodes (D_x in Fig. 3 (a)), electrically interconnected as shown in Fig. 3 (b). Such devices are equally shared between two direct copper bonded (DCB) substrates (DCB 1 and DCB 2 in Fig. 3 (a)). The DCB substrates are soldered on a common AlSiC base plate. Metal-bars, also visible in Fig. 3 (a), implement a pairwise connection between the DCB substrates.
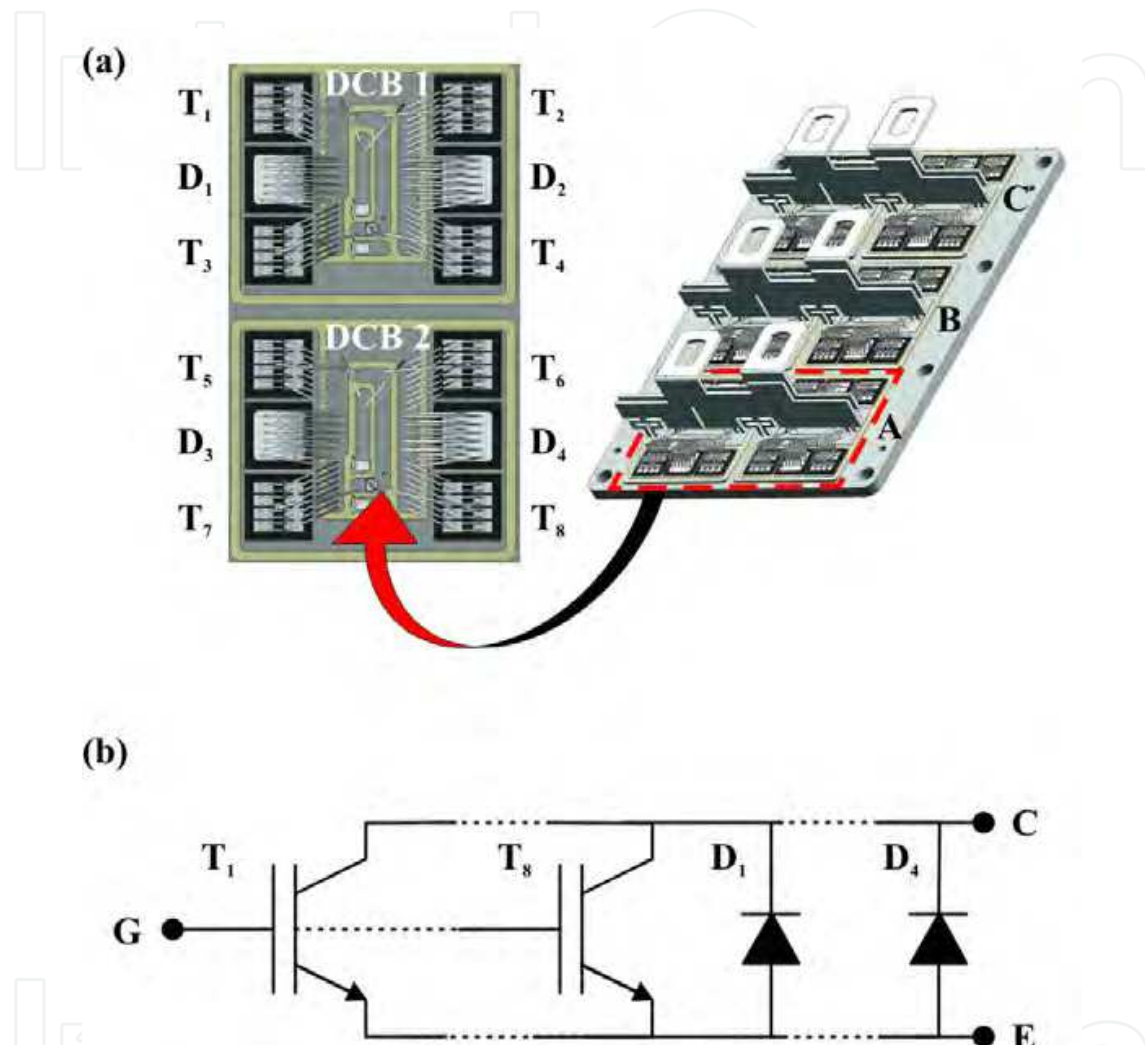

Fig. 3. (a) Power module internal view, showing all the elementary phases and providing a major detail in one of them. (b) Schematic showing the devices connection in one phase and highlighting the terminals: Gate (G), collector (C) and emitter (E).

3.2 Failures of semiconductor power devices in railway traction scenario

The power semiconductor devices most commonly used in railway traction are IGBTs (acting as switches) and diodes (acting as rectifiers). The main difference between them is that the former are switched-off and –on by an external control signal (low power driver), whereas the latter depend on circuit variables. Their role in ERTCs is to control the current flow within the power converter (forward state) and sustain the voltage when the current is diverted to another place (blocking state), e.g. another converter leg (Mohan et al., 1995).

In a railway power inverter, such power devices are always working in switching operation with an inductive load. This can give rise to very stressful processes in terms of instantaneous dissipated power during both the diodes reverse recovery and the IGBTs turn-off, i.e., ruggedness failures when high current and high voltage levels coexist (Perpiñà et al., 2010a). Besides, IGBT modules are also the most sensitive elements to other system failures. For instance, dysfunctions on the IGBT drivers (Bouscayrol et al, 2006; Steimel, 2004), on the sensing elements to monitor the critical electrical and thermal variables of the inverter (Bose, 2006), on the cooling system (Baumann et al., 2001), and on the capacitors (decoupling or filter) (Malagoni-Buiatti et al., 2010) undoubtedly lead to their destruction (induced-failures). Furthermore, their working conditions can be more adverse when the IGBT power module wears out (Lhommeau et al., 2007), a non-optimum thermal management design has been carried out (Perpiñà et al., 2007a, 2010b), and external electrical dysfunctions occur (Malagoni-Buiatti et al., 2010). As mentioned before, the package degradation limits the power converter lifetime since the working temperature inside the module increases due to the solder fatigue among the material stack used for the power module manufacturing (Ciappa, 2002; Mermet-Gunyennet et al., 2007). This ageing process can be enormously accelerated as a consequence of a non-optimum thermal management design (e.g., cooling system design or thermal interface selection) (Perpiñà et al., 2007a). On the other hand, it has been observed that several failures depend on the switching strategy of the power device. Sometimes, the dysfunctions on the driver induce abnormal events (short-circuit, over-current, or over-voltage), which severely stress the components (Khargekar, 1994). However, such events not only result from driving anomalies, but also can be linked to environmental or load conditions (Perpiñà et al., 2007a). In this failure scenario, it is interesting to determine "a posteriori" the device failure signature so as to derive precious information about the device failure origin. Over the years, this analysis has been tackled in both diodes and IGBTs, providing a physical insight into the failures occurred during the diode reverse recovery and the IGBT turn-off under inductive loads (Perpiñà et al., 2010a). Obviously, the working conditions for such components can be more adverse when the power module wears out by thermal fatigue, as can be inferred from their derived failure mechanism explained in the next subsection.

3.3 Failure mechanisms in multi-chip modules aged by thermal fatigue

ERTCs manufacturers should fix at least, a long-term warranty of 30 years. During this long period of time, the main problems present in railway power modules are related to their wear-out. Although several efforts have been addressed to improve the power device ruggedness under overloading conditions, the package wear-out will always be the limiting factor for long-term reliability. For this reason, they follow several accelerated ageing tests not only targeted to the devices or materials performance degradation (e.g., leakage current, gate dielectric, humidity), but also for determining the thermomechanical impact on the material stack conforming the power module (long-term failure mechanisms). Concerning the thermomechanical effect on the power module wear-out, it can be divided into two contributing effects: power devices local dissipation and external temperature variation. Both will exert thermal cycles on the material stack of the package assembly producing the so-called thermal fatigue. The term fatigue comes from the material mechanics field and refers to a cyclic load on a material stack (Pecht, 1991). There are two different tests to explore the thermomechanical induced wear-out of power modules: thermal and power

cycling. As mentioned, the former submits the whole module to uniform temperature swings, whereas the latter considers the local overheating performed by the devices. For the packaging technology previously outlined, PCTs have put in evidence the following failure mechanisms (Ciappa, 2002): reconstruction of metallization, wire-bonding fatigue, and solder alloys fatigue. They are briefly revised in the next subsection, leaving the concept of PCTs to be treated further on.

3.3.1 Reconstruction of metallization

Power cycles induce important periodical compressive and tensile stresses on the device upper metallization because of its large thermo-mechanical mismatch with silicon. As a result, such stresses can undergo far beyond the elastic limit, and their relaxation can occur by mechanical processes (e.g., diffusion creep, grain boundary sliding, or by plastic deformation through dislocation glide) (Ciappa, 2002). This leads either to the extrusion of the aluminium grains or to cavitation effects (empty cavities formation) at the grain boundaries depending on the texture of the metallization, which give rise to the aluminium reconstruction and results into an increase of its sheet resistance with time. Then, it can be monitored by measuring the voltage drop across the device on-state.

3.3.2 Wire-bonding fatigue

Under working conditions (high current ratings and switching operation), wire-bondings are exposed to almost the full temperature swings imposed by both the power dissipation in the silicon and the wire-bonding itself. Moreover, the current density distribution across its section is strongly inhomogeneous due to the skin effect (Ciappa, 2002). In general, the failure of a wire-bonding occurs predominantly as a result of a fatigue caused either by shear stresses generated between the bond pad and the wire-bonding. As a result, they are gradually disconnected from the power devices until they reach the open circuit condition. Two phenomena are observed: crack propagation at the wire-bonding heel (heel cracking propagation) or the lift-off of the wire-bonding (wire-bonding lift-off). In the first case, this problem comes from a non-optimum wire-bonding process which mechanically damages the wire-bonding heel (crack creation). In the latter, the wire-bonding is aged, eventually inducing its lift-off because of the high CTE mismatching between materials. This failure starts at a crack at the tail of the wire-bonding, and propagates through the interface defined between the wire bonding and the chip upper metallization until it completely lifts off (see Fig. 4). The failure evolution can be externally monitored by sensing a change either in the contact resistance or in the internal distribution of the current, such that it can be traced by monitoring the device voltage drop during on state (Cova et al., 1997).

3.3.3 Solder joint fatigue

The main failure mechanism of railway multi-chip power modules is associated with the thermo-mechanical fatigue of the solder joint. The most critical interfaces are the solder joints between the die attach-ceramic substrate and the ceramic substrate-base plate. At such locations one finds the worst CTE mismatching (in both interfaces), the maximum temperature swing combined with the largest lateral dimensions (only for ceramic substrate-base plate). The most frequently used materials as solder joints in multi-chip

power modules are based on tin–silver, indium, or tin–lead alloys (Lutz et al., 2011). They have excellent electrical properties and as soft solders, they exhibit good flow characteristics. Often, solder joints are considered as a single homogeneous phase, but this is not true as their phase evolves with time. For instance, when a material with a copper metallization is soldered with a standard lead–tin alloy, the bond is mainly provided through the formation of a Cu5Sn6 intermetallic phase located close to the copper layer (Ciappa, 2002). Two additional distinct phases, one tin rich and one lead rich, are formed in the central part of the solder joint. During accelerated ageing tests, these phases coarsen rapidly due to the high homologous temperature at which the alloy is operated, experiencing a modification of its thermo-mechanical properties: since the copper phase is much more brittle than the tin–lead phases, thermomechanical fatigue cracks often propagate within the copper rich intermetallic. Due to the larger CTE mismatch and to the higher temperature, fatigue cracks are found preferably in the vicinity of the intermetallic layer immediately below the ceramic substrate. Metallographic preparations have shown that cracks initiate at the border of the solder joint, where the shear stress reaches its maximum (Ciappa, 2002). Additionally, crack formation is highly promoted by the presence of sharp angles at the edges of the ceramic substrate (Ciappa, 2002).
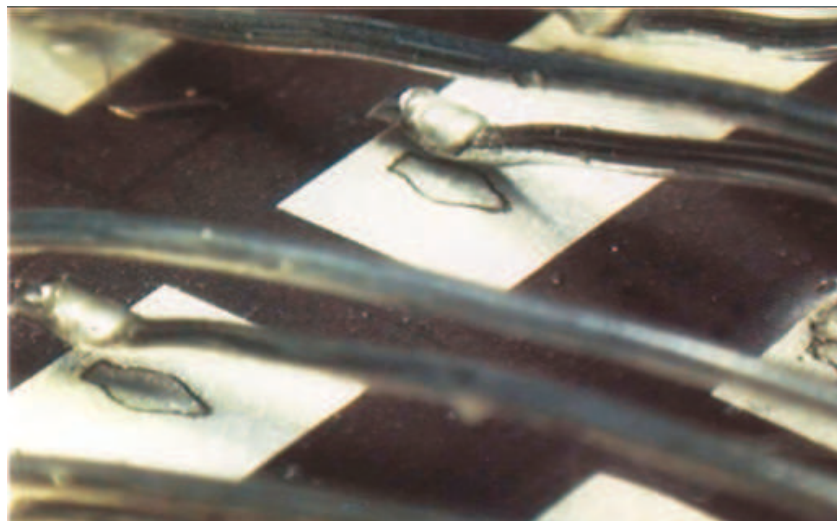

Fig. 4. Wire-bonding lift-off after PCTs

Fig. 5 shows an acoustic microscope image which depicts this behaviour: higher solder delamination (bright areas) is observed at the ceramic substrate edges. The discontinuity at the edges is responsible for a stress peak at this location and especially at the corners. This is due to the fact that attached materials can freely expand with temperature along the unbounded directions, but, at the material attachment interface, they are bonded and their thermo-mechanical properties, mostly the Young modulus and thermal expansion coefficients, will fix the dynamics of the assembly. Therefore, for higher (lower) Young modulus and very different thermal expansion coefficients and material thickness, it is expected to obtain more localized (distributed) strains close to the discontinuity present at edges of the assembly, which will finally induce a higher and more local (lower and more distributed) stress (Ciappa, 2002; Lutz et al., 2011). Therefore, the fractures start at the outside corners and edges and propagate towards the center of the soldered materials, thus absorbing this stored mechanical energy. When a non uniform temperature is observed in

the case of the modules and high temperature gradients are present, the degradation of the solder joint starts at the corners pointing towards the position of the module at which the higher temperature is reached and moves outward. Obviously, several parameters will fix the solder fatigue pattern: the thermal interface between the power module and cooling device, the cooling device design (e.g., water or heat-pipe based), and the base plate backside flatness (Perpiñà et al., 2007b).
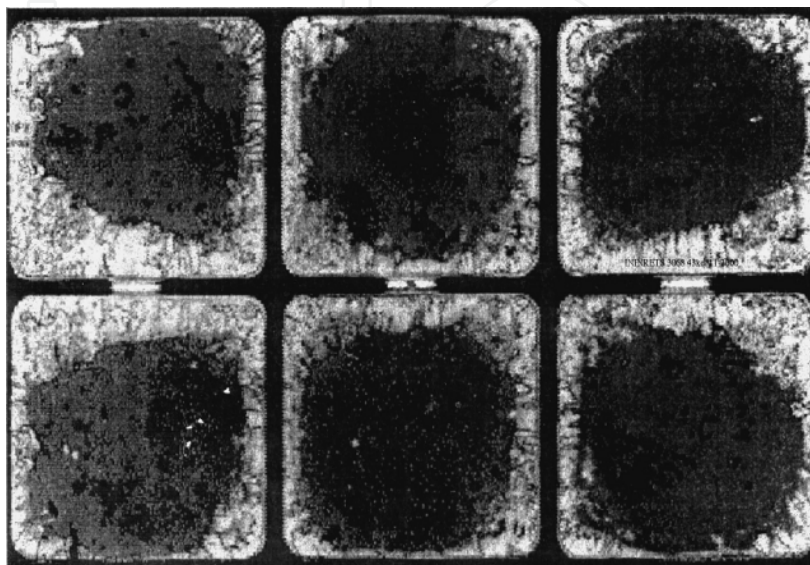

Fig. 5. Solder delamination inside IGBT 3300V 1200A with copper base-plate after 40 Kcycles.

4. Critical revision of lifetime prediction approach in traction modules

In actual IGBT power modules, its lifetime calculation is based on deriving a reference curve obtained when the modules are submitted to local thermal stresses. This curve depicts the number of cycles to failure versus temperature swing (thermal load) at an indicative temperature of the thermal cycle (maximum, average or minimum value), as performed in mechanical fatigue of materials (number of duty cycles to failure versus mechanical load) (Ciappa, 2002). This curve is derived by following accelerated ageing tests representative of the final application (PCTs), in which the die provokes local thermal cycles within the module structure (see Subsection 4.2). For lifetime calculation, a virtual experiment is carried out to extract the thermal cycles (temperature swings) responsible for the thermal fatigue experienced by each constitutive element of the package. They should be computed considering a mission profile representative of a real service line and should be properly counted following an adequate algorithm. Therefore, the current flow and voltage drop across the module are modelled for a given motor and service line. Finally, it is supposed that only an average of all thermal cycles experienced by the module along a service line will contribute on the module ageing to compare such a result with the reference curve. The key points related to its lifetime calculation, the followed procedures, and their limitations are critically discussed in the following subsections. First of all, Subsection 4.1 presents the lifetime methodology, and after Subsections 4.2, 4.3, and 4.4 critically revises the limitations present in PCTs, local temperature measurements in power modules, and the counting and superimposition of thermal cycles, respectively.

4.1 Current followed methodology

The starting point for lifetime prediction in railway power modules is determining a duty cycle based on a train service line (mission profile). Several approaches are possible:

- for trains with a well known mission profiles, like metros or tramways, it is considered the total duty cycle on a given service line assuming maximum load conditions;
- for trains without well defined mission profiles, it is defined a reference duty cycle corresponding to the most stressed course for the train;
- for high speed trains and locomotives, it is very difficult to define a reference cycle.

The key aspect in the above approach is that we only consider thermal cycles in the second timescale (package timescale), which will be referred as traction-braking cycles. Long thermal cycles, like day-night or season cycles, are not considered. In the same way, very short cycles (below second scale) are not accounted for, as they will consider the device or IGBT module-only thermal dynamics without taking into account the effect of the cooling system (Berg & Wolfgang, 1998). For instance, this is the case of statoric cycles at very low speed in locomotives.

In order to determine the thermal cycles experienced by the IGBT modules, several calculations are required. Starting from the cinematic of the train, currents in the motors are estimated. Subsequently, in accordance to the control strategy applied on the converter, the current and voltage ratings seen by the IGBT modules are inferred. At this stage, with the static and dynamic characteristics of IGBT modules, losses at die level (both, IGBTs and Diodes) are estimated. Such losses are the input data for temperature cycle estimation, but another key parameter of the power converter is required: its equivalent thermal model.

Generally, this equivalent model is extrapolated from thermal measurements and is presented under the form of a compact thermal model based on a RC stacking (Foster or Cauer representation) (Ciappa, 2005). These equivalent models are used to calculate the virtual junction temperature (T_{vj}) of the whole IGBT module for diodes and IGBTs. In fact, T_{vj} is an average temperature of the module among all IGBTs or diodes. In a 3.3 kV-1200A IGBT power module (see Fig. 3 (a)), T_{vj} for IGBT (diodes) is the average temperature for 24 chips (12 chips). At this point, we obtain the curve T_{vj} versus time for both IGBT and diode dies (see Fig. 6 (a)), T_c versus time for the power module, and a criterion (detailed in 4.4) to translate these curves into a histogram of cycles, as shown in Fig. 6 (b) (Ciappa, 2000).
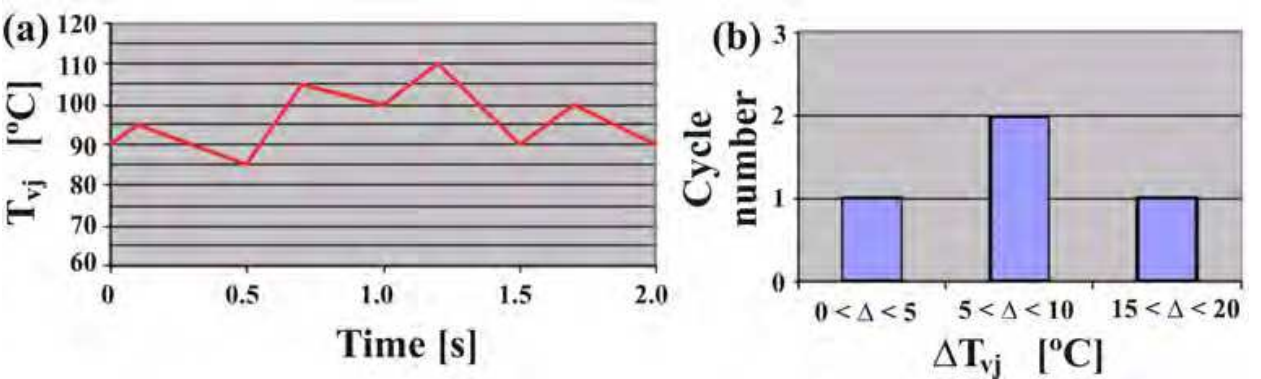

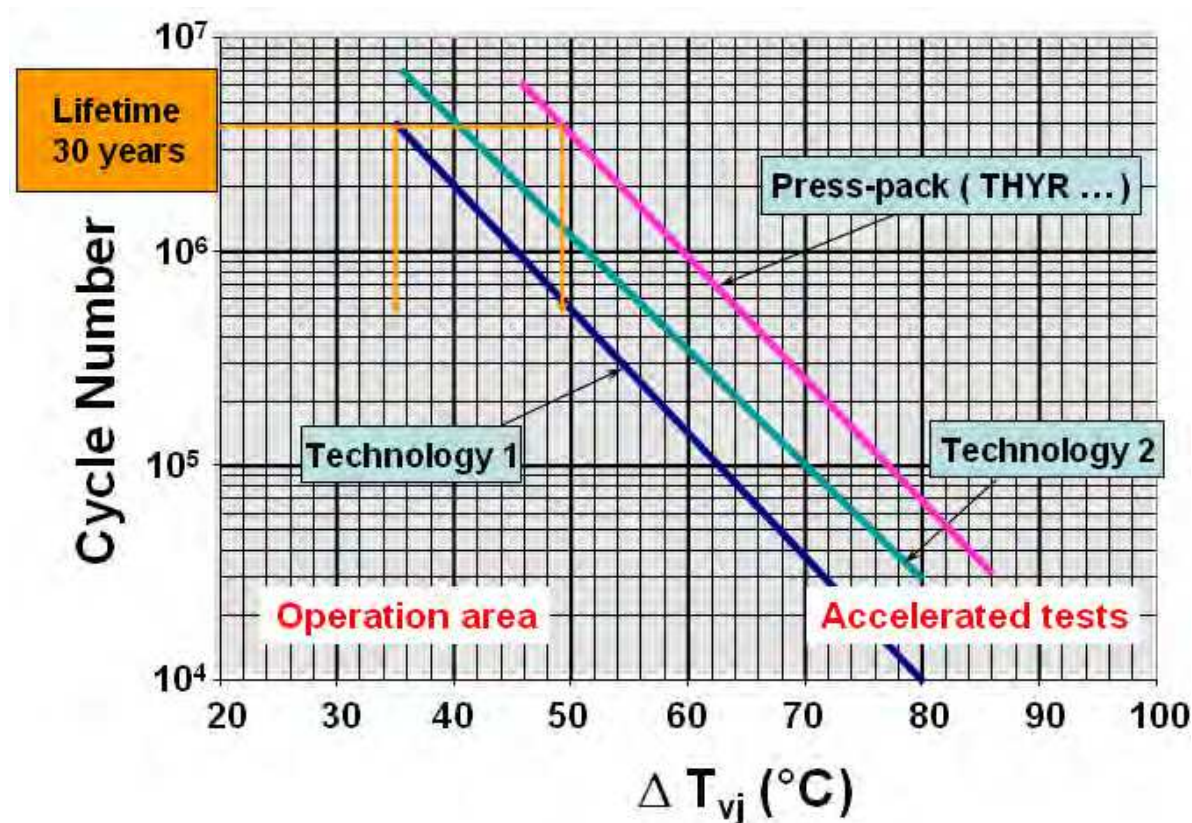Fig. 6. (a) Thermal cycles versus time and (b) histogram of the thermal cycles.

Fig. 7. Reference curves N cycles to failure versus virtual junction temperature cycles for various technologies

The final step is to compare the histogram of thermal cycles obtained for the whole life of the train (example shown in Fig. 6 (b)) with the reference curves for lifetime prediction. Such reference curves correspond to the dependence of the number of cycles to failure N_f versus the amplitude of thermal cycles (temperature swing) experienced in average at die level (ΔT_{vj}), usually by IGBTs. For instance, Fig. 7 shows one of these reference curves: N_f versus ΔT_{vj}. Both reference curves are obtained from PCTs and an extrapolation law based on plastic deformation fatigue (Coffin-Manson-like approximation).

This law assumes that when ΔT_{vj} ranges from 5 to 80°C, the number of cycles until failure N_f may be expressed as:

$$N_f = \lambda \times (\Delta T_{vj})^{-\alpha_{vj}} \times \exp[E_{a,vj}/(k_B T_{vj,m})] \tag{1}$$

where λ and α_{vj} are fitting constants depending on the material mechanical properties, α_{vj} ranging from 5 to 6. Concerning the exponential term (Arrhenius effect), $E_{a,vj}$, k_B, and $T_{vj,m}$ are the activation energy, the Boltzmann constant and the average temperature of the thermal cycle, respectively. It has also been observed in other scenarios that there are other parameters which fix these kind of curves when performing PCTs, such as: heating up time, current and voltage ratings, and wire-bonding diameter. Incorporating such new variables in a new expression inspired in Eq. (1) has led to definition of a more complex law (CIPS model) which allows performing more accurate lifetime predictions. However, this modified expression is no longer valid in traction (Lutz et al., 2011), since it has been settled for Al_2O_3 substrates and not for AlN and AlSiC (as it is the case of traction modules).

In order to compare multiple thermal cycles determined along a given mission profile N_{mp} (see Fig. 6) with the reference curves (N_f versus ΔT_{vj}, se Fig. 7), an equivalent point of the mission profile test should be determined. First of all, an equivalent temperature increase ΔT_e is defined and corresponds to ΔT_{vj} of the histogram at which more cycles have been detected. After, a cumulative cycle to failure N_e at ΔT_e is computed assuming that every thermal cycle consumes a fraction of power module lifetime given by reference curve N_f, i.e.:

$$N_e\,(\Delta T_e) = N_f\,(\Delta T_e) \times \sum_{i=1}^{n} \left(N_{mp}(\Delta T_{vj,i}) \big/ N_f\,(\Delta T_{vj,i}) \right) \tag{2}$$

where i is a subindex which varies within the range of temperatures of the histogram and $\Delta T_{vj,i}$ represents the temperature swing for each one of the considered points in the histogram. In such a calculation, $N_{mp}(\Delta T_{vj,i})$ corresponds to the thermal cycles experienced by the module during 30 years, considering the number of mission profiles performed along this time. The criterion to know if we meet the lifetime requirement is made by placing the derived equivalent point (N_e, ΔT_e) with respect to the considered reference curve and by checking if N_e is lower than the number of cycles of the reference curve at ΔT_e.

4.2 Role of power cycling tests in traction lifetime prediction

As previously mentioned, RAPSDRA program proposed the sketch of reliability tests called active Power Cycling Tests or PCTs (Berg & Wolfgang, 1998). The advantage of these tests in comparison with the followed until then (thermal cycling) was that they considered the local thermomechanical stresses induced by dies dissipating power. These tests are run with IGBT modules mounted on a water-based cooling system (water plate). In order to simplify the test set up, the power module is locally heated by only IGBT devices, which are switched on with a low voltage power supply. The temperature swing is adjusted with the device conduction time (heating up time) and the current level. This means that during PCT, the stress conditions are completely different from real conditions: no switching, no high voltage, no dynamic losses are considered.

In order to determine the end of life of aged modules, a statistical treatment of the experimental results is carried out according to the Weibull statistics (Lutz et al., 2011). Such a statistical criterion gives the number of cycles after which 10% of the modules have reached the end of life. The main criterion for the end of life is the evolution of saturation voltage of the IGBT module $V_{CE,sat}$ (or forward voltage for diodes). A commonly accepted limit is 5%. In the case of monitoring the junction to case thermal resistance, the main criterion is defined as 20% increase. However, such accelerated ageing tests do not provoke the same failure mechanisms than in real conditions and we only observe indicators of the following failure mechanisms:

- collector-emitter saturation voltage for IGBT,
- forward voltage for diode,
- collector-emitter leakage current,
- loss of control of the gate,
- loss of power connections.

There is no clear relation between the evolution of these indicators and the failure mechanisms in the field. A first conclusion on PCT is that they are well adapted to compare durability of wire-bondings and soldering technology, but the extrapolation of PCT tests for lifetime estimation is not so straight-forward. For this reason, the PCT should be redesigned on the basis of the following principles, more oriented to the final application:

- accelerated ageing tests must induce the same failure mechanisms than in real service,
- ageing of packaging structure induces thermal failure mechanisms linked with high voltage and/or switching,
- ageing of packaging is mainly activated by active and passive thermal cycles, and
- distribution of temperature between chips inside the power module is a key factor for inducing a catastrophic failure.

Therefore, not only a thermal stress should be induced, but also the IGBT module should be electrically operated under real working conditions (high voltage and switching) to be representative of the failure observed in the final application. Besides, the cooling conditions for the IGBT power module must be the same than in real service operation.

This is the reason why new tests covering these misleading points should be carried out. They should consist in mounting power modules with inverter legs in a back to back configuration (high current and voltage) and driven by control boards (PWM pattern) modulating the package heating time in order to adjust ΔT_{vj} at 80°C and 60°C. Obviously, the cooling conditions will be the same than in real operation. In order to exactly know the context of the induced failures, current and voltage tracking should be made. These tests should be carried out with at least 10 IGBT modules in order to get a good estimation of the Weibull shape factor of the failure distribution at a given ΔT_{vj}. Then, acceleration factor should be calculated between different ΔT_{vj} under the condition that the same range of Weibull shape factor is maintained whatever is ΔT_{vj}. Unfortunately, this kind of studies have not been already reported in the literature for IGBT power modules for railway traction, only finding a pioneering work in automobile traction (Smet et al., 2011). This work has performed ageing tests with 600 V-200 A IGBT power modules under high voltage and PWM driving conditions. Their parameters have been set in a reference temperature of 60°C with a heating up time of 30 s long. They have observed that wire-bonding and upper metallization degradations are the predominant ageing mechanisms in the case of high thermal stresses (ΔT_{vj}=100°C reaching a maximum junction temperature of 160°C), whereas in the case of less stress-inducing protocols (ΔT_{vj}=60°C reaching a maximum junction temperature of 120°C), the aforementioned failure modes (i.e., wire-bonding fatigue, metallization reconstruction and solder delamination) occur simultaneously. This difference is due to the fact that such stressing conditions generate local thermal stresses at a higher frequency than in PCT conditions, which locally acts on the upper part of the device and reveal different effects.

In any case, PCTs does not allow accessing to a thermal mapping of the IGBT module in thermal working conditions (just monitoring points as detailed in such works). This is a key point for a better understanding of the thermal distribution inside the module and the local thermal cycles generated by the devices and understanding their failures.

4.3 Module thermal distribution measurements

Temperature monitoring at chip level is mandatory to understand what occurs when power devices fail, since it is a key parameter in all processes previously explained. For an individual die, such issue can be easily tackled by means of several approaches based on (Bouscayrol et al., 2006): device thermo-sensitive electrical parameters (TSPs), temperature sensor monolithic integration in the device, thermo-optical techniques. Depending on the spatial resolution, one may define the junction temperature concept, which consists in an average temperature inside the device. However, multi-chip packaging introduces an apparent limitation on temperature local monitoring, since multiple devices are connected in parallel leading to temperature spatial resolution problems. Consequently, an average temperature measurement of all devices is always performed (Bose, 2006). Since any sensing method inside the package has not been envisaged by the manufacturers, usually TSPs are used for power cycling purposes, such as the $V_{CE,sat}$ at low current level (Coquery, 2003).
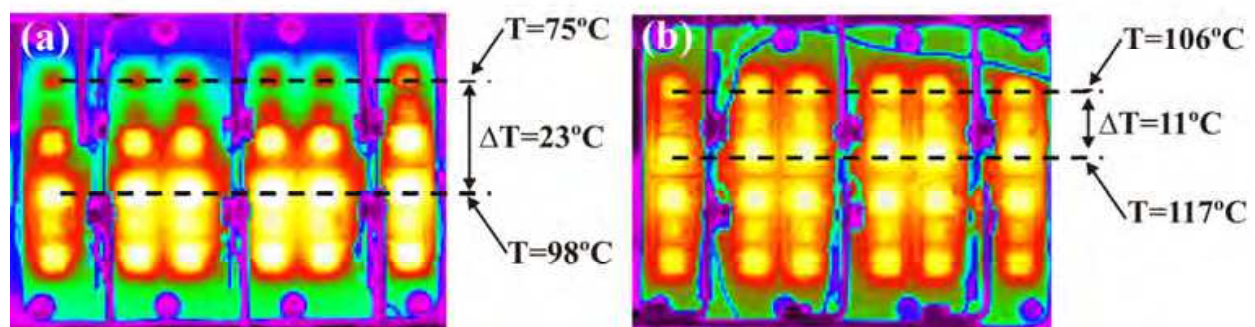
Fig. 8. Infrared thermal mappings of the same module when cooled down by a heatpipe-based thermosyphon (a) or a water cooled-based system (b). They have been performed by measuring first thermal mappings biasing IGBTs and diodes separately (1.8 kW in IGBTs and 0.6 kW in diodes) and after applying the superposition principle.

It has been observed that an uneven temperature distribution inside the module is induced by the module-cooling system interface, the chips placement inside the module, and the module mechanical mounting procedure (Ciappa, 2005; Perpinya et al., 2007c). This can induce a huge temperature dispersion, which leads to more stressed devices depending on their location inside the module. Therefore, determining such temperature distribution becomes essential when facing reliability studies. Fig. 8 depicts this dependence on the heat exchange system employed for cooling down the IGBT module. In this case, a non-optimal forced-convection heat pipe-based thermosyphon (a) and a water-based cooling system (b) are compared, in which the air and inlet water temperatures are 25ºC and 60ºC, respectively. In both measurements, the thermal interaction among other modules is also taken into account. The thermal mappings have been derived in two steps. The thermal mappings referred to each device type are firstly acquired by using 60 s long power pulses (1.8 kW in IGBTs and 0.6 kW in diodes), and afterwards, they are synchronised and added, according to the sources superposition principle (Mohan et al., 1995a). From these thermal mappings, it is clearly evidenced that the commonly followed way to tackle the thermal design of a converter only considering the virtual junction is not the most reliable approach.

4.4 Counting and superimposition of thermal cycles

Commonly, the Rainflow Method (Bannatine et al., 1990) is the most employed, easy to use and practical criterion for stress cycle counting. It consists in an algorithm that transforms the stress (or temperature) curves versus time into a frequency histogram of cycles number versus stress amplitude (or temperature) cycles and stress average value (or temperature) for the cycle. It is also used to measure the likely impact of the most damaging stress cycles in fatigue studies. On the contrary, to the observed thermal cycles in automotive applications (Ciappa et al., 2003), the rainflow method is applicable in railway scenario; because their mission profiles present simple waveforms and their acceleration-braking cycles can be well distinguished. In addition, this method is fairly easy to implement in a computer code, is capable to filter noisy data, and determines the minimum, average, and maximum temperature values of the cycle. Usually, this data is stacked in groups of 5°C, since it has been observed that this small amount of temperature has not an important effect on lifetime prediction and serves as a filtering criterion to make groups of cycles for the derived histogram. When the equivalent point N_e and ΔT_e is extracted for its comparison with the reference curve N_f-ΔT_{vj} obtained from PCT tests, there are some misleading points in all this procedure:

- large cycles are not taken into account (day-night, season cycles),
- temperature swing of the analysed cycles have a linear cumulative effect on the module ageing, i.e., two cycles with a temperature swing of 20 °C have the same effect on the packaging ageing than one cycle of 40°C,
- reference curve should be based on physics based models rather than statistical approaches without fixing a standard procedure to perform PCT tests (e.g., fixing a heat up time or using a cooling system representative of the final application)

5. Mission profile-based approach for local thermal cycles measurement

On the basis of the limitations of the lifetime prediction method explained in section 4, the last part of this chapter proposes an experimental approach for determining local thermal cycles within a power module. This is faced by means of a thermal test bench, in which the actual thermal working conditions of multi-chip power modules are emulated. The main objective is determining how the cooling system and the thermal interface locally affect the temperature distribution inside the module, eventually inferring the thermal cycles at chip level (both diodes and IGBTs). This approach contrasts with the most commonly adopted solutions based on either averaged temperature measurements on the power module by thermo-sensitive parameters (TSPs) (Su et al., 2002) or locally monitoring the temperature at the interface between the set module-cooling system with thermocouples (Coquery et al., 2003). Moreover, this solution is less complex and more straightforward than those explained in 4.2, becomes complementary to accelerated ageing tests, and also evidences the impact of non-uniform thermal distributions inside the package on the long-term reliability of the power inverter. The proposed procedure is carried out on new designs of cooling systems (forced-convection heat pipe-based thermosyphon) to study their suitability for railway applications. First of all, Subsection 5.1 introduces the thermosyphon cooling systems. Next, the details about the used experimental set-up and mission profile computation are outlined in Subsections 5.2 and 5.3, respectively.

5.1 Thermosyphon cooling system description

Generally speaking, a thermosyphon cooling system refers to a method of passive heat exchange based on natural convection, in which circulates a liquid (coolant) in a closed-loop circuit without requiring an external pump. This strategy simplifies the coolant pumping and the heat transfer by avoiding the cost, operation reliability, and complexity problems linked to conventional liquid-pumping systems (Baumann et al., 2001). One particular case of these cooling systems is the convection-forced heat pipe-based thermosyphon investigated in this work (see Fig. 9). It is formed by several sealed tubes which contain a certain amount of coolant, usually methanol pure or mixed with water (heat pipes). The heat pipes are partially inserted in a copper block (evaporator), and the rest are covered by thin fins to facilitate the thermal exchange by air-forced convection (condenser), as depicted in Fig. 9. The IGBT modules are screwed on both sides of the evaporator (see Fig. 9), simultaneously cooling down two legs of one power inverter (two modules per side). This cooling solution is used in railway inverters belonging to the power range from 500 kW to 1000 kW (medium power range), in which the power dissipation requires higher cooling performances than dry panels cooled by air-forced convection, but lower than water pumping-based cooling systems (Baumann et al., 2001).
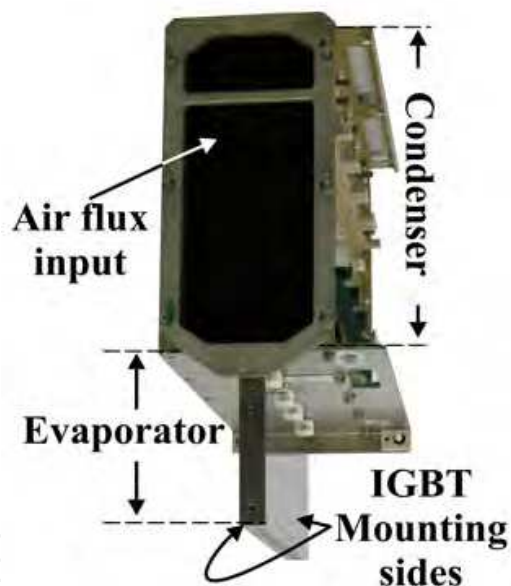
Fig. 9. Photograph of the inspected heat pipe-based cooling system detailing its main parts.

The proper operation of this cooling system relies on the fact that the coolant is located at the evaporator and the condenser is cooled down by air-forced convection. In these systems, the heat removal is produced as follows: the coolant absorbs the thermal energy dissipated by the power module until inducing its evaporation (first phase change). Subsequently, the coolant migrates to the condenser due to the presence of a thermal gradient. At the condenser, the coolant condenses (second phase change) releasing the thermal energy to the air flux. Afterwards, the coolant flows back to the evaporator through the internal wicks present in the walls of the heat pipe cavity (film evaporation process), mainly assisted by capillary forces (coolant pumping effect) (Dunn & Reay, 1983; Romestant, 2000).

5.2 Experimental set-up and thermal test conditions

The thermal interaction between the module and the cooling system has been studied on 3.3 kV-1.2 kA IGBT modules shown in Fig. 3 (a). The naming criterion for the devices and locations also obey to that depicted in this figure; i.e: elementary phases (A, B, and C), DCB substrates (DCB 1 and DCB 2 in Fig. 3 (a)), and devices (IGBTs and diodes T_x and D_x, respectively).

The thermal behaviour of the set module-cooling system is analysed with the set-up detailed in Fig. 10. In this set-up, the thermal interaction between two legs of one inverter is characterised. The approach consisted in inspecting two opened modules (M_3 and M_4) screwed on one thermosyphon side (one inverter leg) by an infrared camera, while the other two modules (M_1 and M_2) are also operating. The opening process of the modules M_3 and M_4 has been carefully performed maintaining their initial static electrical characteristics. No modifications have been introduced on the other two modules M_1 and M_2. The modules have been interconnected in series to a current source to bias them with a given current waveform I_{bias}, thus dissipating any kind of power profile in the analysed thermal system (see Fig. 10 (a)). With this interconnection scheme, the gate-to-emitter voltage in IGBT devices is maintained all the time at 15 V. In this approach, the selected power profile has a time resolution in the hundreds of millisecond range, neglecting the possible effects on the set module-cooling system due to the instantaneous power dissipated under switching operation. In fact, this approximation perfectly allows analysing the inverter long-term reliability, since the thermal performance degradation occurs within the heating up time-scale (second range) of the set module-cooling system (Smet et al., 2011; Yun et al., 2001). The modules have been thermally excited by current instead of power waveforms, as the voltage evolution with the temperature must be ensured to be much closer to the actual working conditions.
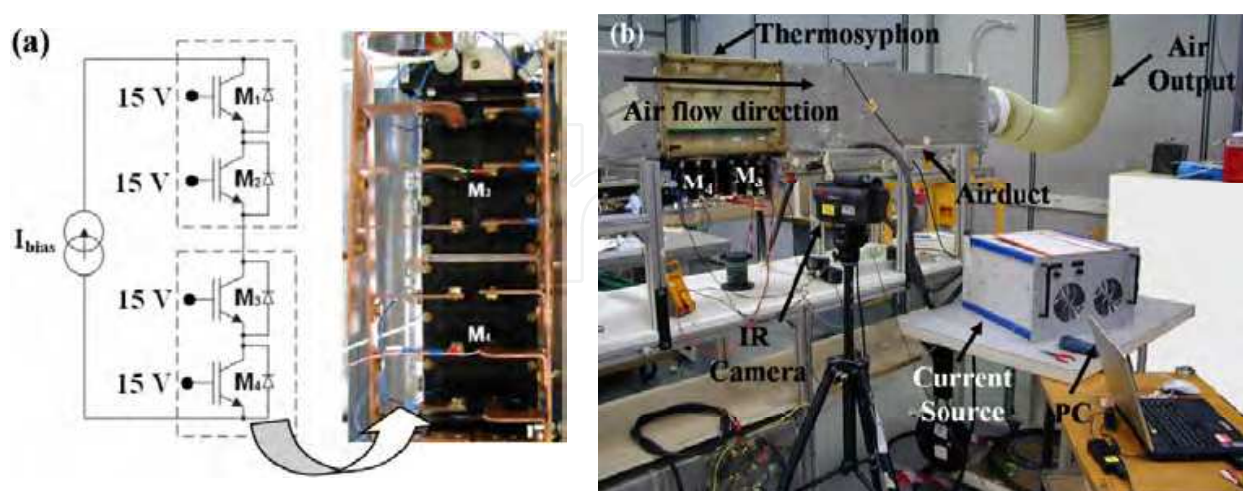

Fig. 10. (a) Circuit schematic showing the connections between the modules. The opened modules are also highlighted. (b) Experimental set-up used for testing the thermosyphon, in which the infrared camera, the airduct, the current source, and the monitoring PC are highlighted.

Fig. 10 (b) presents a photograph of the experimental set-up, highlighting the infrared camera, the current source driven by a computer, and the thermosyphon with the inspected modules. The modules have been screwed on the evaporator in such a way that for each elementary phase, IGBTs and diodes are identified according to their position in the evaporator as Fig. 3 (a) depicts; i.e., the lowest subscript shown in Fig. 3 (a) corresponds to the upper position in the evaporator. The thermal coupling between diodes and IGBTs within the same package can also be inferred from the experimental results. The thermal mappings referred to each type of device are firstly acquired, and afterwards, they are synchronised and added, according to the sources' superposition principle mentioned in 4.3 (Franke et al., 1999; Necati, 1993). Obviously, it is a first approximation to the real thermal mapping under actual working conditions. However, this approach allows us to perform a very good assessment of the whole system local thermal performances, and to predict the base plate-DCB solder delamination, as shown further on. These phenomena have been often analysed assuming an average virtual junction temperature inside the module, resulting in a non interesting approach when performing reliability prediction studies (Ciappa et al., 2003; Khatir & Lefebvre, 2004; Yun et al., 2001).

5.3 Railway service line mission profile determination

In order to obtain a representative mission profile for the power dissipation, the conduction and switching losses are numerically inferred in diodes and IGBTs separately by means of a traction drive design tool called CITHEL (CInematic THermal ELectric) (CITHEL, n.d.; Kreuawan, 2008). Given the route profile, train speed, and motor torque, CITHEL calculates the kinematics and electric aspects at inverter level for a given train characteristic. Thus, the traction chain performances as a function of different electrical motors, power components, and available inverters can be analysed and compared in a very early design stage. CITHEL is a fast solver capable to perform easy iterative calculations in electrical steady state, but it is not an electrical simulator. Unfortunately, this is the only way to estimate P_{total}, since no experimental data are currently available due to the complexity of measuring such a parameter in a real service line. With this software, the power module losses are determined on the basis of IGBT and diode parametric models extracted from experiments at 125°C (component temperature limit). The total power losses (P_{total}) are determined at each calculation time considering both conduction (P_{cond}) and switching ($P_{switching}$) contributions. Exactly, both electrical parameters are averaged over one statoric period, which is a function of the train instantaneous speed (Mohan et al., 1995a). P_{cond} is extracted from (Baliga, 1996):

$$P_{cond} = V_0 \times I_m + R_d \times I_{ef}^2 \qquad (3)$$

where V_0 makes reference to the knee voltage and R_d is the on-resistance of the device. As a first approximation, the on-state of both devices, IGBT and diode, is modelled by a static characteristic defined by two straight lines that join at V_0, whose slopes are zero and R_d, respectively. I_m and I_{ef} refer to the average and effective current supplied to the motor for one statoric period, respectively. On the other hand, by assuming a sinusoidal output current resulting from the considered PWM scheme (Pulse Width Modulation) (Holmes et al., 2003), $P_{switching}$ is calculated as (Mohan et al., 1995a):

$$P_{switching} = F_s \times \sum_{i=1}^{n} E_i \tag{4}$$

where E_i corresponds to the energy loss due to the turn-on or -off, i counts each event indistinctly, and n represents the total number of turn-on and -off events during one statoric period. The diode turn-off losses are neglected in CITHEL computations. E_i has been experimentally related to the instantaneous current when a turn-on or -off event occurs (I_i), which can be written as (Mohan et al., 1995a):
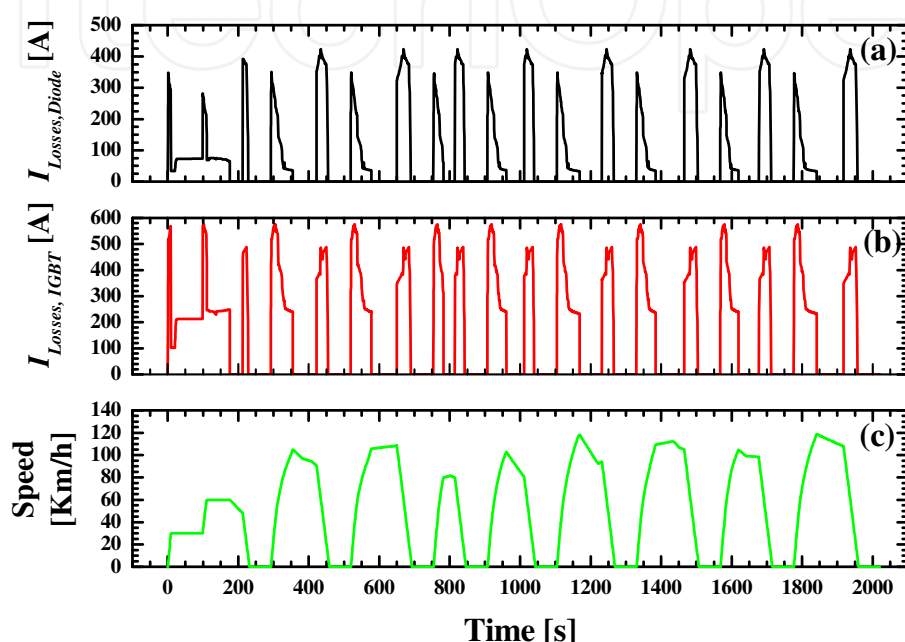

Fig. 11. I_{Losses} used to reproduce the dissipated power corresponding to switching and conduction losses for IGBTs (a) and diodes (b) extrapolated from behavioural models, as well as the speed required along a half of the service line (c).

$$E_i = V^{\alpha} \times \left(a\, I_i + b\, I_i^2 + c\, I_i^3 \right) \tag{5}$$

in which V is the line voltage (input voltage); α, a, b, and c are fitting parameters extracted from experiments. I_i can be easily determined by the following expression (Mohan et al., 1995a):

$$I_i = I_{Amp} \times \sin\left(2\pi\, i \frac{F_{stator}}{F_{switching}} \right) \tag{6}$$

where I_{Amp} is the amplitude of the resulting sinusoidal current waveform, F_{stator} denotes the motor statoric frequency, and $F_{switching}$ gives the modulation frequency associated with the followed PWM scheme (Mohan et al., 1995a). Regardless of the several limitations dealing with the performed time average, CITHEL is capable to calculate the P_{total} evolution at the second time-scale. Thereby, the contribution of the thermal effects due to the package and cooling system will be accounted for. The obtained mission profile can be used for reliability estimations, in spite of the simplicity of the used models, especially to infer P_{cond}.

Finally, the required current profile is analytically inferred from CITHEL results by using the measured I-V characteristic of the considered modules at 125°C. On the basis of a real route profile, Fig. 11 illustrates for a half of the service line, the derived current mission profile for both devices, IGBTs ((a), $I_{Losses,IGBT}$) and diodes ((b), $I_{Losses,Diode}$), and the speed profile (c). The total service line duration is 90 min (5400 s.). In this case, the speed profile has been selected to follow the theoretical maximum speed permitted along the service line.

6. Experimental results

Section 6 presents the main results derived from the approach detailed in the previous section. Subsection 6.1 shows how the proposed test bench allows the determination of the device with the highest thermal stress during real acceleration-braking cycles. Subsection 6.2 depicts that the most delaminated areas in the DBC-solder interface correspond to both the location of the most stressed components and the presence of a higher thickness of thermal interface material (non uniform distribution). Besides, this subsection correlates these results to those obtained with IGBT modules with a copper base plate aged with endurance cycling tests. Such tests have consisted in connecting two inverters in a back to back configuration (high voltage and current), which reproduces the real operation of power modules in PWM driving conditions.

6.1 Local thermal cycles measured on devices

From the followed experiments, several interesting results have been obtained at package and cooling system level. Figs. 12 (a) and (b) illustrate the inferred temperature mappings for each device between two consecutive stations at the end of the train acceleration and braking processes, respectively. This temperature distribution is representative of the real thermal mapping of the module for a time-scale in the second range. Therefore, a first experimental estimation of the thermal interaction of the module with its cooling system is extracted in the worst case (acceleration or braking cycles), which clearly evidences the temperature dispersion among the dies. Under these conditions, the maximum temperature differences are reached. Fig. 12 also evidences a clear vertical temperature gradient due to the chosen cooling system. At first sight, the temperature in the module M_3 is higher than in M_4 (around 10°C). This fact is a direct consequence of the air heating by M_4, when the heat exchange is produced within the thermosyphon condenser region. Moreover, the DCB 2 of phase B within module M_3 suffers the highest thermal stress during real acceleration-braking cycles.

Fig. 13 illustrates the inferred temperature evolution T_{IGBTs} (see Fig. 13 (a)) of four representative IGBTs in M_3 (see Fig. 13 (b)) during a part of the mission profile, considering the thermal interference with the diodes. Fig. 13 (a) shows 20°C temperature differences between dies from M_3. This fact could be attributed to two possible effects related to the cooling process. First, once the liquid has been heated up and the evaporation process starts, a pressure difference inside the heat pipe (at the evaporator) is induced, which in turn, introduces a temperature gradient within the heat pipe (Dunn & Reay, 1983). In the second case, the turning liquid (i.e., coolant) in the wick coming back from the condenser has a higher efficiency in cooling down the chips T_1 and T_3 (upper position) than T_5 and T_7, because of the liquid level inside the tube. As a consequence, chips T_1 and T_3 are cooled down by film evaporation process (the real heat pipe working principle); whereas the other ones follow a pool-boiling heat exchange mechanism (Dunn & Reay, 1983; Romestant, 2000).
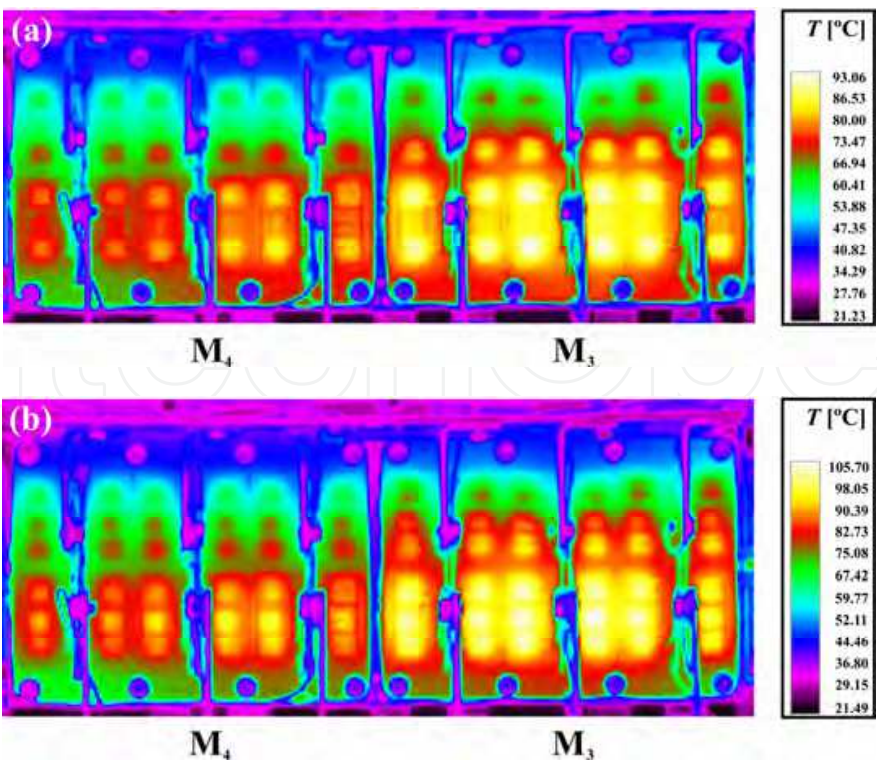
Fig. 12. Infrared thermal mappings of the power modules at the end of an acceleration (a) and braking (b) process shown in Fig. 11, considering the thermal interaction between diodes and IGBTs (not at the same colour scale).
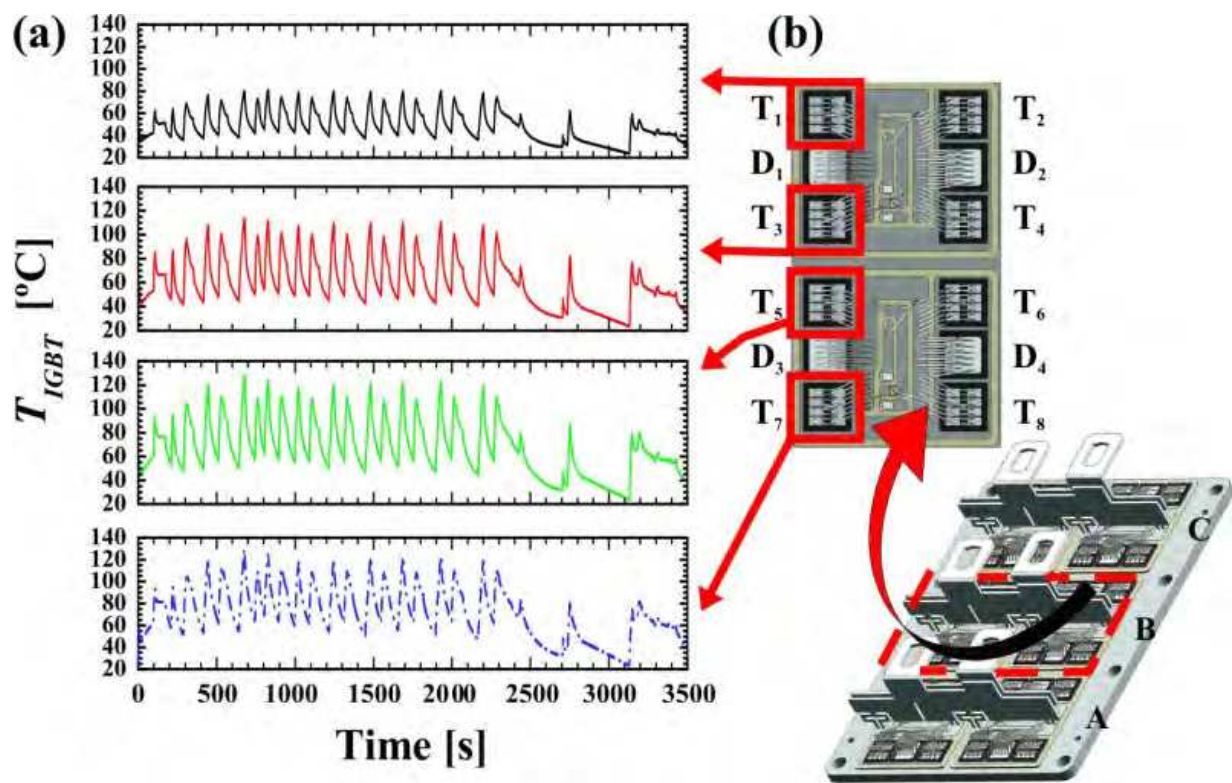

Fig. 13. (a) Junction temperature of four IGBTs (T_{IGBT}) in the same module taking into account the thermal interaction with diodes. (b) IGBTs under study.

Another remarkable fact observed in Fig. 13 (a) is the high temperature swing experienced by the chips (up to 65ºC) due to the slow thermosyphon dynamic response. Such behaviour can be expected, since heat pipes must be heated up to be efficiently operative. This point is very important, since the module wear-out is very sensitive to the temperature swing (Ciappa, 2002).

In order to compare and summarise the temperature information shown in Fig. 13 (a), the thermal cycles experienced by each die have been counted by following the rainflow method and classified according to their temperature swing ΔT_{cycle} and the reached temperature peak T_{peak}. T_{peak} has been selected instead of T_m, because this variable provides us an idea of the maximum temperature reached by each IGBT. The ΔT_{cycle} class is divided into fourteen categories going from 5ºC to >65ºC in steps of 5ºC, and T_{peak} is distributed into six sets going from 40ºC to 140ºC in steps of 20ºC. Fig. 14 presents the thermal cycles experienced by the four selected IGBTs in M_3. The most (less) stressed set corresponds to the highest (lowest) T_{peak} and ΔT_{cycle} values. It can be observed from Fig. 14 that the thermal stress is distributed differently among chip T_1 and the other dies, which is in accordance to the remarks related to Fig. 13 (a). Fig. 14 also demonstrates that chip T_5 experiences the most stressing thermal cycles. Therefore, an asymmetrical wear-out effect on the module is expected to occur at long-term.

6.2 Effects of local thermal cycles on thermal grease and solder

Fig. 15 show the thermal grease distribution originated from the experienced thermal cycles, when the power modules M_3 and M_4 are removed. Fig. 15 (a) is obtained when the air flux goes from M_4 to M_3, whereas Fig. 15 (b) is originated from performing twice the mission profile changing at each time the air flux direction. Fig. 15 (a) presents that the coldest module (M_4) has attached more thermal grease than the hottest one (M_3). In the case of Fig. 15 (b), one can observe a similar grease distribution. This result highlights how from a certain temperature value, the thermal grease liquefies, improving the thermal contact of the module. By capillary effects, the thermal grease fills in the voids of the module-cooling system interface. However, this eventually leads to the thermal grease to be displaced observing that it has been partially or completely removed (thermal interface degradation). This indicates that a good measure for maintenance would be replacing the thermal grease after some working time.

Fig. 16 (a) depicts the DCB solder delamination observed in a module (M3 position), which comes from an endurance test performed on the analysed cooling system. In a back to back configuration by using two inverters, they have been operating to obtain the solder delamination observed in Fig. 16 (a). This process has been carried out on modules that have a copper base plate. The reason to select such modules is that a high degree of delamination in the solder DCB-base plate can be obtained with few thermal cycles (Ciappa, 2002). This result is compared with the solder delamination results obtained in a previous work (Khatir & Lebefvre, 2004), where classical power cycling tests were performed to induce the module wear-out (see Fig. 16 (b)). In that case, the module was cooled down by a water-pumping based cooling system. One may observe from both figures that the solder delamination patterns are different. Fig. 16 (a) presents a DCB substrate with a higher solder delamination in the zone where Fig. 12 shows higher temperature values during both acceleration and braking processes (DCB 2 corresponding to the phase B of M3). On the contrary, Fig. 16 (b) presents a higher solder delamination at the centre of the module, coinciding with the region where the module has the worst thermal contact to the cooling system (Perpiñà et al., 2007a).
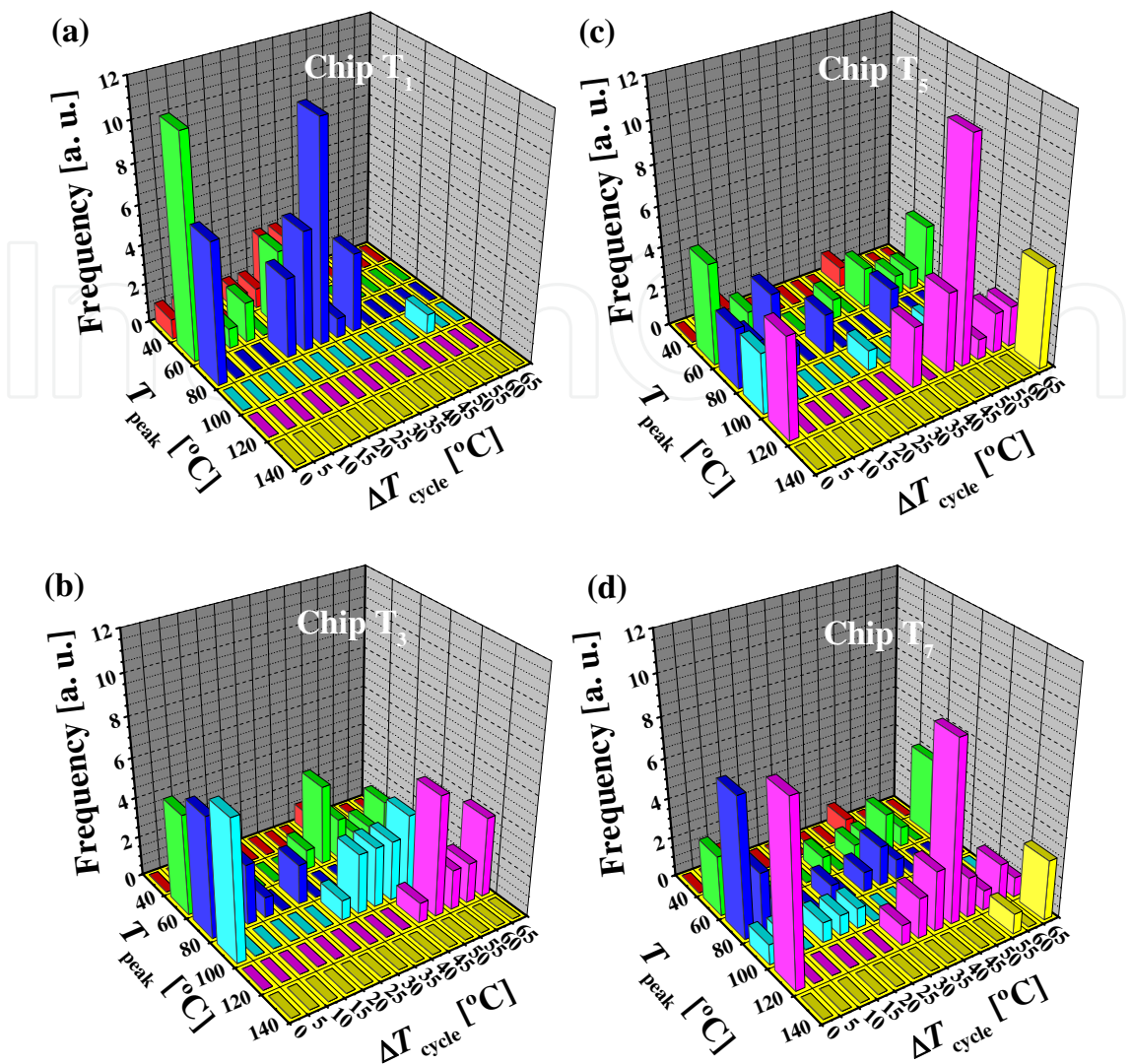
Fig. 14. Number of temperature cycles experienced by the four IGBTs shown in Fig. 13 (b), counted by means of the rainflow method: (a) Chip T_1, (b) Chip T_3, (c) Chip T_5, (d) Chip T_7.
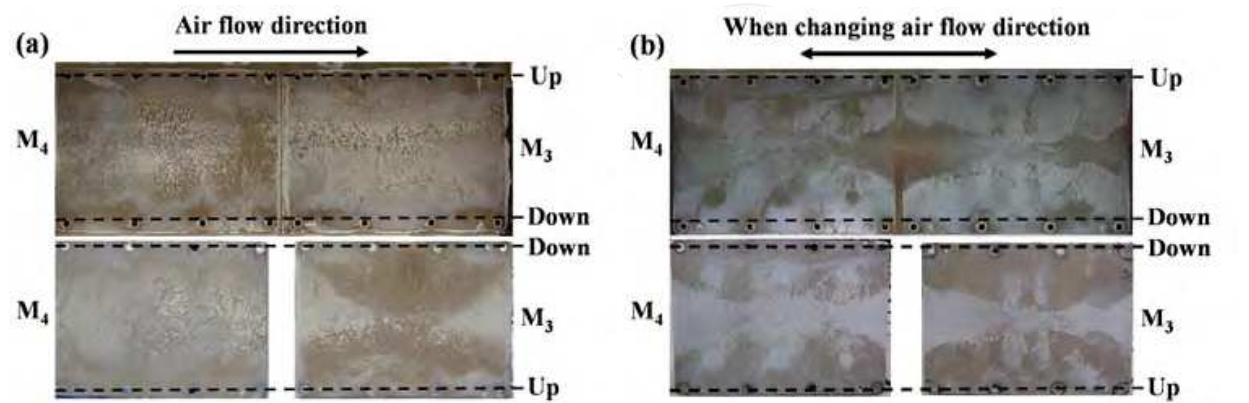

Fig. 15. Thermal grease distribution on both the modules and cooling system resulting from the local thermal cycles after a mission profile in two different conditions: (a) when a single mission profile is effectuated maintaining the same air flow direction, (b) when the mission profile is repeated twice and changing the air flow direction.
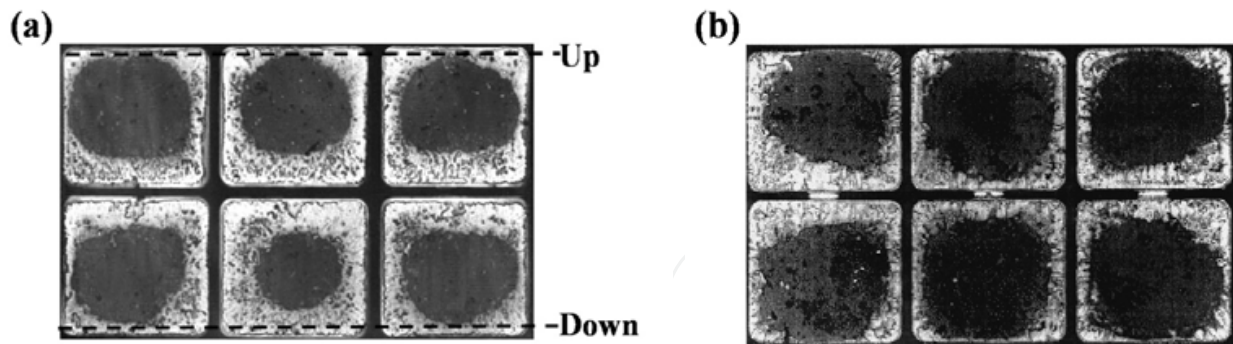
Fig. 16. Base plate-DCB solder delamination observed in IGBT modules with copper base plate, when cycled in a heat pipe (a) or water pumping-based (b) cooling systems.

7. Conclusions

Packaging wear-out of IGBT modules is one of the main limiting factors for ERTC long-term reliability. They are mainly due to the thermal cycles originated from the power devices working conditions across the package structure and the mismatch between its constitutive materials. This leads to crack initiation and propagation across the package interfaces or solder joints, which degrade the thermal performance of the package.

For this reason, the final user has developed a procedure to determine the IGBT module lifetime. After reviewing this methodology, it is evidenced that the results obtained are not representative of the failures observed from the field. In fact, they are representative for the manufacturer interest to improve its product, but not for the final user. Several times, the harsh environmental conditions or the real working conditions, both electrical and thermal, could induce a device failure before to the predictions given by only considering an ageing process. Therefore, it is crucial to link the failure criteria of Power Cycling Tests ($V_{CE,sat}$, $R_{th,j-c}$, leakage current) to real electrical failure mechanism. For this reason, new tests covering these misleading points should be carried out. They should consist in mounting power modules in inverter legs in a back to back configuration (high current and voltage) and driven by control boards (PWM pattern) modulating the package heating time in order to adjust ΔT_{vj} at 80ºC and 60ºC and considering the cooling conditions in real operation. Some comments have also been addressed to some misleading points on the methodology followed for thermal cycles superimposition. In this procedure, some approximations are taken into account: large cycles are not considered (day-night, season cycles) and temperature swing of the analysed cycles have a linear cumulative effect on the module ageing. Moreover, lifetime prediction reference curves should be based on physics based models rather than statistical approaches without fixing a standard procedure to perform PCT tests (e.g., fixing a heat up time or using a cooling system representative of the final application).

At the end of this chapter, the impact of the interaction between the power module and its cooling system on the inverter reliability is analysed. This study is mainly based on an air-forced convection heat pipe-based thermosyphon. The thermal mapping is experimentally determined and the non uniform temperature distribution inside the power module is justified by the special characteristics of the cooling system. Moreover, a comparison of the

temperature dispersion between devices within the power module with a water-based cooling system is also provided. The local thermal cycles obtained from a real mission profile are measured, and their effects on solder delamination and thermal grease degradation are indicated. Finally, these results are compared with some features observed on failed power modules coming from the field, both being in agreement.

8. Acknowledgment

9. References

Arnold, E.; Pein, H. & Herko, S. (1994). Comparison of self-heating effects in bulk-silicon and SOI high voltage devices, *Proceedings of International Electron Device Material (IEDM)*, San Francisco (USA), pp. 813-816, 1994.

Baliga, B.J. (1996). *Power Semiconductor Devices*, PWS Publishing Company, Boston, MA, 1996, ISBN: 0-534-94098-6.

Bannantine, J.; Comer, J. & Handrock, J. (1990). *Fundamentals of Metal Fatigue Analysis*, New Jersey, Prentice Hall, 1990, ISBN: 0-133-40191-X.

Baumann, H.; Heinemeyer, P.; Staiger, W.; Töpfer, M.; Unger, K. & Müller, D. (2001). Optimized cooling systems for high-power semiconductor devices, *IEEE Transactions on Industrial Electronics*, vol. 48, no. 2, pp. 298-306, April 2001, ISSN: 0278-0046.

Berg, H. & Wolfgang, E. (1998). Advanced IGBT Modules for Railway Traction Applications : Reliability Testing. *Microelectronics Reliability*, Vol. 38, pp. 1319-1323, 1998, ISSN: 0026-2714.

Bose, B.K. (2006). Power electronics and motor drives recent progress and perspective, *IEEE Transactions on Industrial Electronics*, vol. 56, no.2, pp. 581-588, April 2006, ISSN: 0278-0046.

Bouarroudj, M.; Z. Khatir, J-P Ousten, S. Lefebvre (2008). Temperature-level effect on solder lifetime during thermal cycling of power modules, *IEEE Transactions on Device and Materials Reliability*, vol. 8, no. 3, September 2008, ISSN: 1530-4388.

Bouscayrol, A.; Pietrzak-David, M.; Delarue, P.; Peña-Eguiluz, R.; Vidal, P-E. & Kestlyn, X. (2006). Weighted control of traction drives with parallel-connected AC machines, *IEEE Transactions on Industrial Electronics*, vol.53, no. 6, pp. 1799-1806, December 2006, ISSN: 0278-0046.

Ciappa, M. & Fichtner, W. (2000). Life-time Prediction of IGBT Modules for Traction Applications. *Proceedings of International Reliability Physics Symposium (IRPS)*, San Jose (California, USA), 2000.

Ciappa, M. (2002). Selected failure mechanisms of modern power modules, *Microelectronics Reliability*, vol. 42, no. 4-5, pp. 653-667, April/May 2002, ISSN: 0026-2714.

Ciappa, M.; Carbognani, F.; Cova, P. & Fichtner, W. (2003). Lifetime prediction and design of reliability tests for high-power devices in automotive applications", *Proceedings of International Reliability Physics Symposium (IRPS)*, Dallas (USA), pp. 523-528, 2003.

Ciappa, M.; Fichtner, W.; Kojima, T.; Yamada, Y. & Nishibe, Y. (2005). Extraction of Accurate Thermal Compact Models for Fast Electro-Thermal Simulation of IGBT Modules in Hybrid Electric Vehicles, *Microelectronics Reliability*, Vol. 4, issues 9-11, 2005, ISSN: 0026-2714.

CITHEL (n.d), User Manual.

Coquery, G.; Carubelli, S.; Ousten, J.P. & Lallemand, R. (2001). Power module lifetime estimation from chip temperature direct measurement in an automotive traction inverter, *Microelectronics Reliability*, vol. 41, no.9-10, pp. 1695-1700, September/October 2001, ISSN: 0026-2714.

Coquery, G.; Piton, M.; Lallemand, M.R.; Pagiusco, S. & Jeunesse, A. (2003). Thermal stresses on railways traction inverter IGBT modules: concept, methodology, results on sub-urban mass transit application to predictive maintenance, *Proceedings of European Power Electronics and Drives (EPE)*, Toulouse (France), 2003.

Cova, P.; Ciappa, M.; Franceschini, G., Malberti, P. & Fantini, F (1997). Thermal characterization of IGBT power modules. *Proceeding of Microelectronics and Reliability*, Vol. 37, Issues 10-11, pp. 1731–1734, 1997

Dunn, P.D. & Reay, D.A. (1983), *Heat Pipes*, Third Edition, Pergamon Press, Oxford, 1983. ISBN: 0-08041903-8.

Franke, T.; Zaiser, G.; Otto, J.; Honsberg-Riedl, M. & Sommer, R. (1999). Current and temperature distribution in multi-chip modules under inverter operation, *Proceedings of European Power Electronics and Drives (EPE)*, Lausanne (Switzerland), 1999.

Hamidi, A. (1998a). *Contribution à l'étude des phénomènes de fatigue thermique des modules IGBT de forte puissance destinés aux applications de traction*, PhD. Thesis, Institut National Polytechnique de Lorraine (Lorraine, France), 1998.

Hamidi, A.; Coquery, G.; Lallemand, R.; Vales, P. & Dorkel, J.M. (1998b). Temperature measurements and thermal modeling of high power IGBT multichip modules for reliability investigations in traction applications, *Microelectronics Reliability*, vol. 38, no. 6-8, pp. 1353-1359, June/August 1998, ISSN: 0026-2714.

Holmes, D.G. & Lipo, T.A. (2003). *Pulse Width Modulation for Power Converters: Principles and Practice*, IEEE press Series on Power Engineering. Piscataway, NJ:IEEE press, October 2003, ISBN: 978-0-471-20814-3.

Khargekar, A.K. & Kumar, P.P. (1994). A novel scheme for protection of power semiconductor devices against short circuit faults, *IEEE Transactions on Industrial Electronics*, vol. 41, no. 3, pp. 344-351, June 1994, ISSN: 0278-0046.

Khatir, Z. & Lefebvre, S. (2004). Boundary element analysis of thermal fatigue effects on high power IGBT modules, *Microelectronics Reliability*, vol. 44, no. 6, pp. 929-938, June 2004, ISSN: 0026-2714.

Kreuawan, S. (2008). *Modelling and optimal design in railway applications*, PhD thesis, École Centrale de Lille, Lille (France), 2008.

Lhommeau, T.; Perpiñà, X.; Martin, C.; Meuret, R.; Mermet-Guyennet, M. & Karama, M. (2007). Thermal Fatigue Effects on the Temperature Distribution inside IGBT

Modules for Zone Engine Aeronautical Applications, *Microelectronics Reliability*, vol. 47, no. 9-11, pp. 1779-1783, September/November 2007, ISSN: 0026-2714.

Lutz, J.; Schlangenotto, H.; Scheuermann, U. & De Doncker, R. (2011). *Semiconductor Power Devices*, Springer, Heidelberg (Germany), 2011, ISBN 978-3-642-11124-2.

Malagoni-Buiatti, G.; Martín-Ramos, J.A.; Rojas-García, C.H.; Amaral, A.M.R. & Marques Cardoso A.J. (2010). An on-line and non-invasive technique for the condition monitoring of capacitors in boost converters, *IEEE Transactions on Instrumentation and Measurement*, vol. 59, no. 8, August 2010, ISSN: 0018-9456.

Mermet-Guyennet, M.; Perpiñà, X. & Piton, M. (2007). Revisiting power cycling test for better lifetime prediction in traction, *Microelectronics Reliability*, vol. 47, no. 9-11, pp. 1690-1695, September/November 2007, ISSN: 0026-2714.

Mohan, N.; Undeland, T.M. & Robbins, W.P. (1995a). *Power Electronics: Converters, Applications and Design*, Second Edition, J. Wiley & Sons, Inc., April 1995, ISBN: 0-471-22693-1

Necati, M (1993). *Heat conduction*, 2nd edition, John Wiley and Sons, New York, USA, 1993, ISBN: 0-47153256-8.

Pecht, M. (1991). *Handbook of electronic package design*, Marcel Dekker, New York, 1991, ISBN: 0-8247-7921-5.

Perpinya, X.; Garonne, O.; Rochet, J.P.; Jalby, P.; Mermet-Guyennet, M. & Rebollo, J. (2007c). Experimental Analysis of Temperature Distribution within Traction IGBT Modules", *Proceedings of European Power Electronics and Drives (EPE)*, Aalborg (EUA), 2007.

Perpiñà, X.; Castellazzi, A.; Piton, M.; Mermet-Guyennet, M & Millán, J. (2007a). Failure-relevant abnormal events in power inverters considering measured IGBT module temperature inhomogeneities, *Microelectronics Reliability*, vol. 47, no. 9-11, pp. 1784-1785, September/November 2007, ISSN: 0026-2714.

Perpiñà, X.; Serviere, J.F.; Urresti-Ibañez, J.; Cortés, I.; Jordà, X.; Hidalgo, S.; Rebollo, J. & Mermet-Guyennet, M. (2010a). Analysis of Clamped Inductive Turn-off Failure in Railway Traction IGBT Power Modules under Overload Conditions, accepted in *IEEE Transactions on Industrial Electronics*, 2010, ISSN: 0278-0046.

Perpiñà, X., Mermet-Guyennet, M.; Jordà, X.; Vellvehi, M. & Rebollo, J. (2010b). Long-term reliability of railway power inverters cooled by heat pipe-based systems, submitted to *IEEE Transactions on Industrial Electronics*, 2010, ISSN: 0278-0046.

PORTES (2004), *Power Reliability for Traction Electronics* (PORTES), Marie Curie Transfer of Knowledge, MTKI-CT-2004-517224, EU funded project.

Rahimo, M.; Kopta, A., Schnell, R.; Schlapbach, U.; Zehringer, R. & Linder, S. (2004). 2.5kV-6.5kV Industry Standard IGBT Modules Setting a New Benchmark in SOA Capability, *Proceedings of Power Electronics/Intelligent Motion/Power Quality (PCIM)*, Nuremberg (Germany), 2004.

Romestant, C. (2000). *Etudes théoriques et expérimentales de caloducs et de thermosiphons soumis à de fortes accelerations*, PhD Thesis, Université de Poitiers, Poitiers (France), 2000.

Sankaran, V.A.; Chen, C.; Avant, C.S. & Xu, X. (1997). Power Cycling Reliability of IGBT Power Modules, *Proceedings of IAS*. New Orleans (USA), pp 1222-1227, 1997.

Sheng, W.W. & Colino, R.P. (2005). *Power electronic Modules, design and manufacture*. CRC press, ISBN: 0-203-50730-4.

Smet, V.; Forest, F.; Huselstein, J-J.; Richardeau, F.; Khatir, Z.; Lefebvre, S. & Berkani, M. (2011). Ageing and failure modes of IGBT modules in high-temperature power cycling, *IEEE Transactions on Industrial Electronics*, Vol. 58, no. 10, October 2011, ISSN: 0278-0046.

Steimel, A. (2004). Direct self-control and synchronous pulse techniques for high-power traction inverters in comparison, *IEEE Transactions on Industrial Electronics*, vol.51, no. 4, pp. 810-820, August 2004, ISSN: 0278-0046.

Xu, D.; Lu, H.; Huang, L.; Azuma, S., Kimata, M. & Uchida, R. (2002). Research on the power loss and junction temperature of power semiconductor devices, *IEEE Transactions on Industrial Applications*, vol. 38, no. 5, pp. 1426-1431, September/October 2002, ISSN: 0093-9994.

Yun, C-S.; Ciappa, M.; Malberti, P. & Fichtner, W. (2001). Thermal Component Model for Electrothermal Analysis of IGBT Module Systems", *IEEE Transactions of Advanced Packaging*, vol. 24, no. 3, pp. 401-406, August 2001, ISSN: 1521-3323.
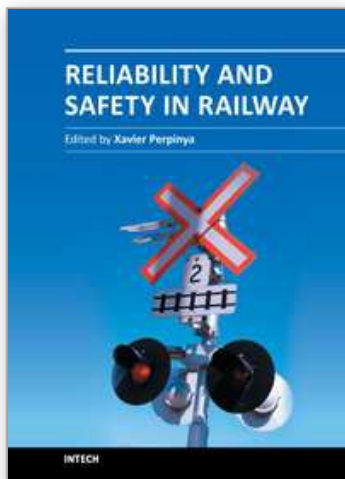
Reliability and Safety in Railway

Edited by Dr. Xavier Perpinya

In railway applications, performance studies are fundamental to increase the lifetime of railway systems. One of their main goals is verifying whether their working conditions are reliable and safety. This task not only takes into account the analysis of the whole traction chain, but also requires ensuring that the railway infrastructure is properly working. Therefore, several tests for detecting any dysfunctions on their proper operation have been developed. This book covers this topic, introducing the reader to railway traction fundamentals, providing some ideas on safety and reliability issues, and experimental approaches to detect any of these dysfunctions. The objective of the book is to serve as a valuable reference for students, educators, scientists, faculty members, researchers, and engineers.

How to reference

In order to correctly reference this scholarly work, feel free to copy and paste the following:

INTECH
open science | open minds